

This Page Is Inserted by IFW Operations
and is not a part of the Official Record

BEST AVAILABLE IMAGES

Defective images within this document are accurate representations of the original documents submitted by the applicant.

Defects in the images may include (but are not limited to):

- BLACK BORDERS
- TEXT CUT OFF AT TOP, BOTTOM OR SIDES
- FADED TEXT
- ILLEGIBLE TEXT
- SKEWED/SLANTED IMAGES
- COLORED PHOTOS
- BLACK OR VERY BLACK AND WHITE DARK PHOTOS
- GRAY SCALE DOCUMENTS

IMAGES ARE BEST AVAILABLE COPY.

**As rescanning documents *will not* correct images,
please do not report the images to the
Image Problem Mailbox.**

REMARKS

Reconsideration of the application is requested in view of the remarks below.

Rejections Under 35 USC 103

The Office Action rejected Claims 10-14 on the grounds that they were clearly anticipated by XP-000874467 (Alonso). The rejection should be withdrawn in view of the remarks below.

The rejection should be withdrawn. It is well settled that to establish a *prima facie* case of obviousness, the USPTO must satisfy all of the following requirements. First, the prior art relied upon, coupled with the knowledge generally available in the art at the time of the invention, must contain some suggestion or incentive that would have motivated the skilled artisan to modify a reference or to combine references. *In re Fine*, 5 USPQ2d 1596, 1598 (Fed. Cir. 1988). Second, the proposed modification must have had a reasonable expectation of success, as determined from the vantage point of one of ordinary skill in the art at the time the invention was made. *Amgen v. Chugai Pharmaceutical Co.* 18 USPQ 2d 1016, 1023 (Fed Cir, 1991), cert. denied 502 U.S. 856 (1991). Third, the prior art reference or combination of references must teach or suggest all of the limitations of the claims. *In re Wilson*, 165 USPQ 494, 496, (CCPA 1970). The Office Action did not establish a *prima facie* case of obviousness.

Applicants' Invention relates to a process that makes a tungsten carbide. The process involves gas phase carburization of tungsten powders and/or suitable tungsten precursor compound powders at a temperature ranging from 850°C to 950°C, such that the carburizing gas phase used is a CO₂/CO mixture. The CO₂ content is above the Boudouard equilibrium content corresponding to the carburization temperature. The carburization is carried out with a carbon activity ranging from 0.4 to less than 1. In one embodiment, the carburization is carried out with a carbon activity from 0.4 to 0.9. In another embodiment, the carburization temperature ranges from 900°C to 950°C. In another embodiment, the carburization is carried out at carburization temperature over a period from 4 to 10 hours.

Alonso teaches the production of tungsten carbide (WC) from tungsten trioxide (WO₃) by means of CO-CO₂ mixtures (61, 78 and 100% v/v CO) in the

temperature interval ranging from 700°C to 1100°C (See Abstract). Alonso teaches that between 700 and 800°C, the process was controlled by the nucleation and growth of the lower oxid $W_{20}O_{58}$, whereas between 800 and 1100°C the process was controlled by the elementary reaction $WO_2 \rightarrow W$. Alonso teaches that a second order dependence of the initial rate constant with respect to partial CO pressure was estimated. The thermomechanical data used for the W-C-O system were consistent with the experimental results. Alonso concluded that the most appropriate conditions for the reduction-carburization of tungsten trioxide by means of carbon monoxide-carbon dioxide mixtures were a temperature of 900°C, a gaseous mixture composition of 100% v/v CO, a volumetric flow rate of 1450 ml (STP)/min and a time of 6 hours. Under these conditions, according to Alonso, a tungsten carbide powder with an average particle diameter of 0.40 μm was obtained.

Alonso does not suggest Applicants' invention. An object of Applicants' invention is to provide a process for the carburization of tungsten powders or tungsten precursor powders, which allows fast and complete carburization and also ensures that deposition of free carbon on the produced tungsten carbide is avoided (See Specification, page 2, lines 21-29). Alonso is completely silent about this object and recommends to use solely CO, i.e. to avoid mixtures of CO and CO_2 , a process inevitably resulting in carbon deposition. Reconsideration is requested.

Alonso teaches gas-phase carburization of tungsten trioxide using CO without any CO_2 as well as using CO_2/CO mixtures containing 78 and 61 % by volume of CO, respectively. At a temperature of 900°C the corresponding carbon activities are 0.026 (61 % CO), 0.077 (78 % CO) and essentially infinity (100 % CO), respectively. Applicants have found that such alternatives are disadvantageous. Low carbon activity results in a low reaction rate, whereas a carbon activity being essentially infinity results in deposition of free carbon on the produced tungsten carbide. Reconsideration is requested.

Alonso does not teach other contents of CO. Alonso does not teach other carbon activities. This means Alonso teaches either using a mixture of CO and CO_2 having a very low carbon activity, or completely avoiding CO_2 (carbon activity = essentially infinity). Alonso does teach these two alternatives and does not teach a broad range for the carbon activity as alleged by the Office Action. Reconsideration

Mo-6323

- 3 -

is requested.

B. Rejection of Claim 15 Under 35 USC 103 over Alonso in view of FR 2 294 133

The Office Action rejected Claim 15 under 35 USC 103 over Alonso in view of FR 2 294 133 (FR '133).

Applicants' invention, as encompassed by Claim 15, relates to a process that subjects the tungsten carbide made by the process according to Claim 10 to a heat treatment at a temperature ranging from 1,150°C to 1,800°C after carburization.

FR '133 teaches obtaining WC by treating finely divided WO_3 with CO at a temperature at which no agglomeration or sintering action takes place to effect the following reaction $\text{WO}_3 + 5\text{CO} \rightarrow \text{WC} + 4\text{CO}_2$.

The rejection should be withdrawn. It is known by one skilled in the art that the specific surface area of powders made by thermal decomposition depends on the decomposition temperature. Increasing decomposition temperature results in decreasing specific surface area, i.e. increasing particle size. To support this point, Applicants hereby enclose a copy of the publication entitled "Chemistry of Powder Production," (p. 106-113), which teaches this phenomenon for MgO (Figure 4.15) and BaTiO₃ (See Figure 4.18).

Accordingly, one of ordinary skill in the art would have expected that heat treatment of WC at temperatures higher than the temperature of carburization would result in an increase of particle size of the WC-powder. In case such a powder is used to produce a liquid-phase sintered composite material, e.g., WC-Co (= hard-metal) the degree of dispersion of the WC-phase and hence the hardness of the composite material was supposed to decrease. Surprisingly, Applicants have discovered that is not the case. Instead, Applicants have discovered that the hardness increase (See Table 2, Example 1 (no heat treatment) vs. examples 2, 3 and 5 (heat treatment)) is observed.

The differences between Applicants Invention and Alonso, singly or in combination with Felten, compel the withdrawal of the rejection. Alonso does not teach heat treatment after carburization. The same is true with regard to Felten. Felten teaches that the reaction of WO_3 and C proceeds at a temperature ranging from 1200 to 1500°C, but this is the carburization temperature and not at all a

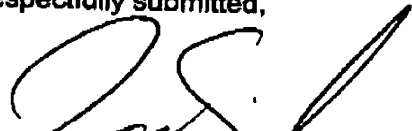
temperature range regarding heat treatment of WC after carburization. Surprisingly, heat treatment according to the invention encompassed by Claim 15 results in material with decreased tendency to secondary grain growth (e.g., to a material with a very homogeneous structure (See page 12, lines 9-11 and Fig. 5 and 6)).

In other words, one of ordinary skill in the art following the teachings of Alonso, singly or in combination with FR '133 would not have been motivated to modify Alonso, practice Applicants' invention, and expect the results Applicants' have obtained.

In view of the foregoing amendments and remarks, allowance of new Claims 10-15 is earnestly requested.

Respectfully submitted,

By



Diderico van Eijk
Attorney for Applicants
Reg. No. 38,641

Bayer Chemicals Corporation
100 Bayer Road
Pittsburgh, Pennsylvania 15205-9741
PHONE: (412) 777-3069
FACSIMILE PHONE NUMBER:
412-777-2612
e-mail: van Eijk/dve0833

Mo-6323

- 5 -

SERIES

POWDER TECHNOLOGY SERIES

CTION

olt in the
ls and

der materials
aracterization
ies of the
ics.

the
owder technology
ials for advanced

this an
and properties
also make it an
gy in general.
n Tokyo and the

CHEMISTRY OF POWDER PRODUCTION

| Arai |



CHEMISTRY OF POWDER PRODUCTION

Yasuo Arai



CHAPMAN & HALL

P O W D E R T E C H N O L O G Y S E R I E S**P O W D E R**

CHEMISTRY OF POWDER PRODUCTION

Yasuo Arai

Powder technology is a wide-ranging subject area that plays an important role in the manufacture of many industrial materials such as pharmaceuticals, materials and agrochemicals.

Chemistry of Powder Production focuses on the solid-state chemistry of powder materials and relates this to the structure and properties as well as preparation and characterization techniques of these important industrial products. Additionally the properties of the particles are discussed in relation to their surface structure and characteristics.

The book describes the fundamentals of statistical methods for measuring the characteristics of particles. New advanced materials being developed via powder technology manufacturing techniques are also emphasized, including powdered materials for advanced ceramics as well as magnetic and pigment materials.

Industrial chemists, chemical engineers and powder technologists will find this an invaluable reference text for dealing with the preparation, characterization and properties of powder materials. It is well illustrated and written in a way that should also make it an ideal introduction to the field of powder production and powder technology in general.

Yasuo Arai is the Professor of Solid State Chemistry at Nihon University in Tokyo and the President of the Society of Inorganic Materials, Japan.

Also available from Chapman & Hall

Particle Size Analysis

Classification and sedimentation methods

I.C. Bernhardt

Hardback (0 412 55880 7), 448 pages

Particle Technology

H. Rumpf (trans. F.A. Bell)

Hardback (0 412 35230 3), 212 pages

Particle Classification

K. Heidkannen

Hardback (0 412 49300 4), 336 pages

Powder Surface Area and Porosity

S. Lowell and Joan E. Shields

Third edition, hardback (0 412 39690 4), 264 pages

CHEMISTRY OF POWDER PRODUCTION

| Arai |



ISBN 0-412-39540-1

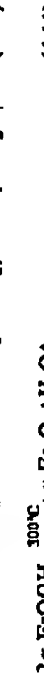
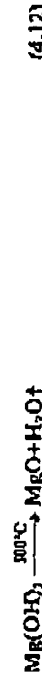


9 780412 395406 >

CHAPMAN & HALL
London · Weinheim · New York · Tokyo · Melbourne · Madras

106 *The preparation of powders*

Typical reactions for the thermal decomposition of these metal salts are as follows:



The above reactions are examples of processes for producing a solid B and vapour C by the thermal decomposition of a solid A:



The thermal decomposition of solid A usually progresses through several stages rather than by a simple reaction. These steps may be thought of as:

1. The release of vapour C from the crystal lattice of solid A, when the increase in temperature causes the vapour pressure of C to rise above 1 atm.
2. The formation of nuclei of B as a new solid phase in the skeletonized lattice of solid A, the available spaces being made by the loss of vapour C.
3. The shrinking of the skeletonized lattice of solid A and development of solid B nuclei.
4. The disappearance of solid A and the further development of nuclei of B to form larger crystals of B.

Particles of B formed through the steps (2) and (3) are produced as submicrometre ultra-fine particles, an order of size impossible to produce by the usual grinding methods. Ultra-fine particles (nuclei) of MgO dispersed in the skeletonized hexagonal lattice of Mg(OH)₂, formed by thermal decomposition by reaction (4.12) are shown as a scanning electron micrograph in Fig. 4.14. This picture corresponds to stage (2) in the sequence above.

The rate of heating is an important factor in controlling the progress of thermal decomposition reactions such as A → B + C. If the thermal decomposition progresses rapidly at a high temperature, numerous nuclei of B are rapidly formed in the skeletonized lattice of solid A and many very fine particles of B are formed by rapid growth. If, on the other hand, the decomposition progresses slowly at the lowest possible temperature, a small number of B nuclei are formed gradually and these nuclei will grow slowly to larger crystals exhibiting characteristic crystal planes. It is difficult, however, to know which type of reaction will occur for any given substance A.

Now we shall consider the thermal decomposition reactions of solids in more detail. The relationships between the weight-loss curves of Mg(OH)₂ by thermogravimetry (TG) and differential thermal analysis (DTA) (with temperature increasing at the rate of $10^\circ\text{C min}^{-1}$) and changes in the specific surface area of Mg(OH)₂ during heating are shown in Fig. 4.15. The structure of Mg(OH)₂ is of the CaF_2 hexagonal type and consists of a layered structure in which layers of Mg and OH are stacked in the order -OH-Mg-OH-OH-Mg-OH-, oriented normally to the direction of the c-axis. The structure cleaves easily between the van der Waals bonded adjacent OH layers, and OH radicals in these layers are easily decomposed by heating. In this decomposition, two layers of OH^- combine and are soon converted to one layer of O^{2-} as shown in the reaction $2\text{OH}^- \rightarrow \text{O}^{2-} + \text{H}_2\text{O} \dagger$. Heat treatment of Mg(OH)₂ at more than 380°C is needed to provide the activation energy required for the diffusion of OH^- ions. From the thermal analysis curves of Mg(OH)₂ shown in Fig. 4.15(h), it is seen that the thermal decomposition of



Figure 4.14 MgO nuclei formed in the skeletonized lattice of Mg(OH)₂. (From V. Arati, *Graswin Line*, 14b, 55 (1971).)

Thermal decomposition of solids 109

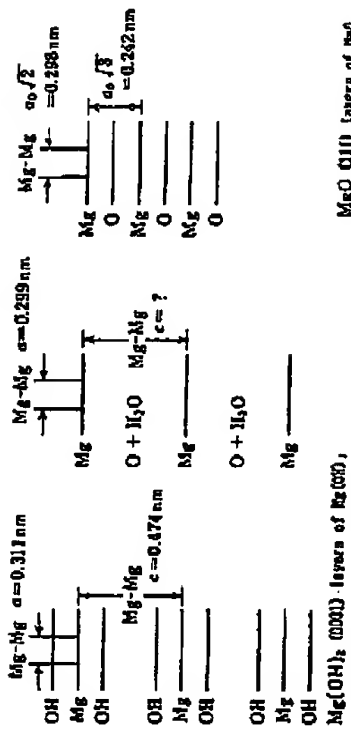


Figure 4.16 Decomposition mechanism of $\text{Mg}(\text{OH})_2 \rightarrow \text{MgO} + \text{H}_2\text{O}$.

First, (1) shows a side view of the (0001) plane in the hexagonal lattice of $\text{Mg}(\text{OH})_2$ before decomposition. The Mg–Mg distance on the (0001) plane is 0.311 nm and that between Mg layers along the c-axis is 0.474 nm. On the other hand, structure (2) shows the side view of the (111) plane in the face-centred cubic lattice of MgO after the decomposition of $\text{Mg}(\text{OH})_2$. The Mg–Mg distance in the (111) plane is 0.298 nm and that between Mg layers is 0.242 nm. Therefore, the (0001) plane of $\text{Mg}(\text{OH})_2$ can be rearranged to the (111) plane of MgO by only a slight decrease of the Mg–Mg distance from 0.311 nm to 0.298 nm when $\text{Mg}(\text{OH})_2$ is converted to MgO . However, the Mg–Mg distance along the c-axis shrinks significantly from 0.474 nm to 0.242 nm as the two layers of OH^- are converted into one layer of O^{2-} by the dehydration of the OH^- layers.

The structures shown in (2) and (3) are of the skeletonized lattice of $\text{Mg}(\text{OH})_2$ formed during the decomposition. Although most of the OH radicals diffuse in all directions as decomposition occurs, the Mg layers remain as they were without a decrease in the interlayer distance in spite of the expulsion of water. Because of this, the Mg layer structure is extremely porous and includes many fine openings, which remain after the release of water. Diffused OH^- released OH^- molecules and O^{2-} remaining after the decomposition of the OH^- will be randomly dispersed between the Mg layers. Structure (4) is found after decomposition of the $\text{Mg}(\text{OH})_2$ is complete. At this stage the dispersed O^{2-} ions converge to form an O^{2-} layer between the Mg^{2+} layers as the (111) plane of MgO , and the MgO crystal structure gradually develops until it shrinks to the normal interplanar spacing of MgO . In this scheme steps (2) and (3) are very active states where ultra-fine particles of MgO are deposited in the

109 The preparation of powders

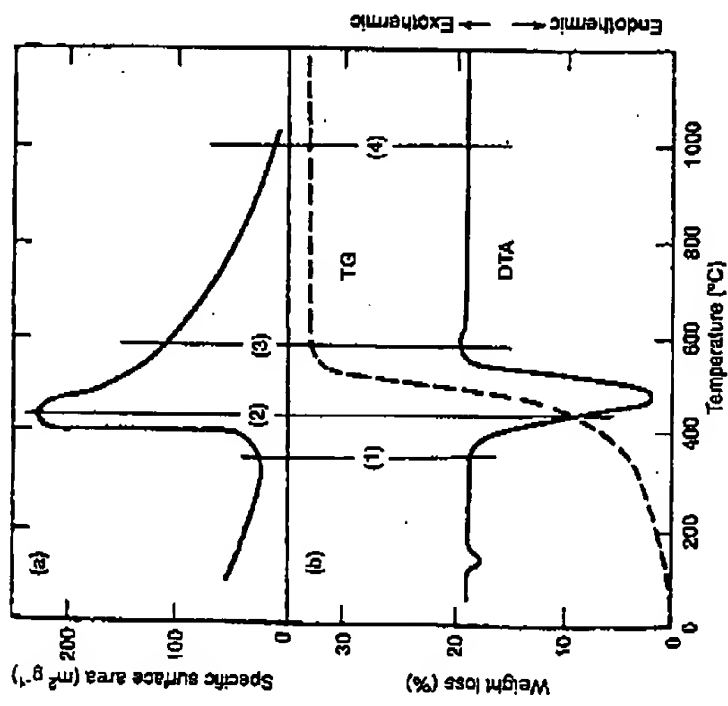


Figure 4.15 Changes in the TG and DTA curves and in the specific surface area of $\text{Mg}(\text{OH})_2$ during heating.

$\text{Mg}(\text{OH})_2$ begins at about 380°C and is complete by about 500°C. A slight endothermic peak appears at about 120°C, which is due to the release of absorbed water trapped between the OH^- layers.

When A is converted into B by thermal decomposition, it is frequently found that the crystalline orientations of the reactant and product are related. Each ion of crystal A will move the shortest distance corresponding to the lowest energy required to form the new arrangement of ions in crystal B. The relationship in orientation between $\text{Mg}(\text{OH})_2$ and MgO is shown in the structural diagram in Fig. 4.16. In that figure, (1), (2), (3) and (4) are the structures occurring consecutively during the stages of heating.

THEIR DECISIONS IN THE MARKET

The changes in specific surface area during stages (1), (2), (3) and (4) are shown in Fig. 4.15(a). From the remarkable increase of specific surface area during stage (2), it is clear that thermal decomposition of $Mg(OH)_2$ suggests itself as a technique for producing ultra-fine grades of MgO . It is not possible to produce these particles by mechanical grinding. The particles produced by thermal decomposition have a very homogeneous structure and uniform size, which gives them very good tinting properties. The thermal decomposition route also avoids the contamination normally found when trills are used.

Figure 4.17 compares the size distributions of Fe_2O_3 powder prepared by the thermal decomposition of $\text{FeS}_4 \cdot 7\text{H}_2\text{O}$ and by the mechanical grinding of natural Fe_2O_3 one. The thermal decomposition product shows ultra-fine particles in the narrow size range from 0.2 to 2 μm whereas the ground product shows a much wider range from 0.5 to 40 μm . If Mn-Zn ferrites are prepared under the same conditions, using both Fe_2O_3 ,

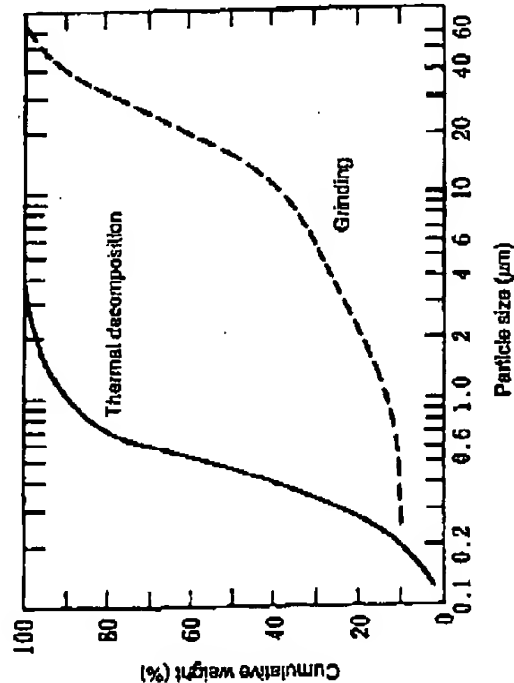
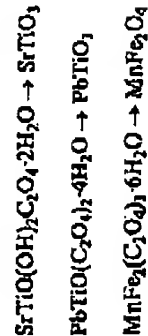


Figure 4.17 Size distributions of Fe_3O_4 powder produced in two ways: synthesis via thermal decomposition of $\text{FeSO}_4 \cdot 7\text{H}_2\text{O}$, and mechanical grinding of natural Fe_3O_4 .

In materials above, the effect of abnormal growth of the particles on the magnetic properties is clearly observed for the ground product. Reaction (4.13) is often used to manufacture BaTiO₃ ceramics for capacitors and is also an application of thermal decomposition. Although the main method for making the sintered body of BaTiO₃ has been by the solid-phase reaction of BaCO₃ and TiO₂ powders, this method has disadvantages, such as the limited size produced by the final grinding of the product and inhomogeneities originating from the initial mixing of the powders. A method for direct production of BaTiO₃ powder was subsequently developed using the solid-phase thermal decomposition route.

Aqueous solutions of high-purity BaCl₂ and TiCl₄ are mixed in the mole ratio of 1.0:1.00, and 2.7 mol oxalic acid solution is gradually dropped into the mixed solution. A soft white precipitate, identified as BaTiO(C₂O₄)₂·4H₂O, is continuously precipitated from the solution. This precipitate converts directly into BaTiO₃ powder through removal of the water of crystallization and subsequent thermal decomposition of the oxalate by heat treatment, as shown in reaction (4.13). BaTiO(C₂O₄)₂·4H₂O as co-precipitated contains Ba:Ti in exactly the atomic ratio of 1:1 and is perfectly homogeneous on the molecular scale.

The changes in specific surface area and particle size of BaTiO₃ powder obtained by thermal decomposition of BaTiO(C₂O₄)₂·4H₂O are shown in Fig. 4-18. Solid-phase reactions between BaCO₃ and TiO₂ in the powder state proceed rapidly at temperatures in excess of 1100–1200°C, but BaTiO₃ begins to be formed at temperatures of around 700°C by the thermal decomposition of BaTiO(C₂O₄)₂·4H₂O. Furthermore the BaTiO₃ particles formed at 700°C are very active and have good sintering properties. On the industrial scale, ultra-fine powdered BaTiO₃ with a particle size of less than 1 μm can be made by the thermal decomposition of the oxalate at 900°C for 4 h. The preparation of ultra-fine powders by the thermal decomposition of co-precipitates is widely used for the preparation of electronic materials such as Pb(Zr,Ti)O₃, MnFe₂O₄, ZnFe₂O₄ and SrTiO₃, as well as for making BaTiO₃. Some examples of reactions making use of the thermal decomposition of oxalates are shown below.



Reaction (4.14) shows the thermal decomposition of α -FeOOH as a way of making γ -Fe₂O₃, which is an important material in the manufacture

112 The preparation of powders

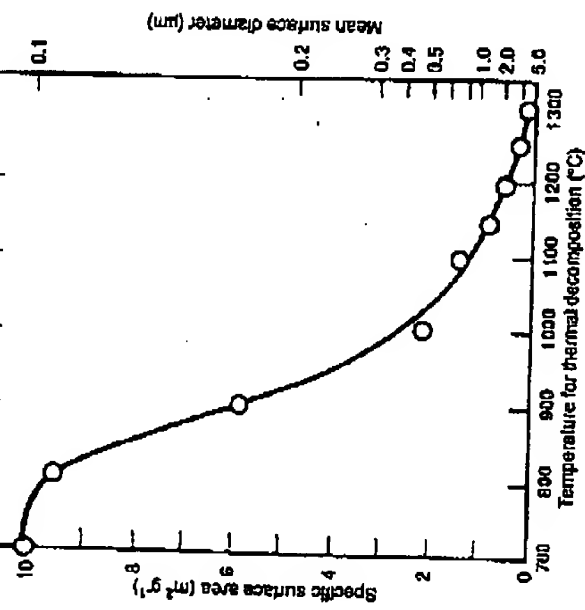


Figure 4.18 Changes in specific surface area and mean surface diameter (assuming spherical particles) of BaTiO_3 powder obtained by thermal decomposition of $\text{Ba}(\text{TiO}_3)_2 \cdot 4\text{H}_2\text{O}$.

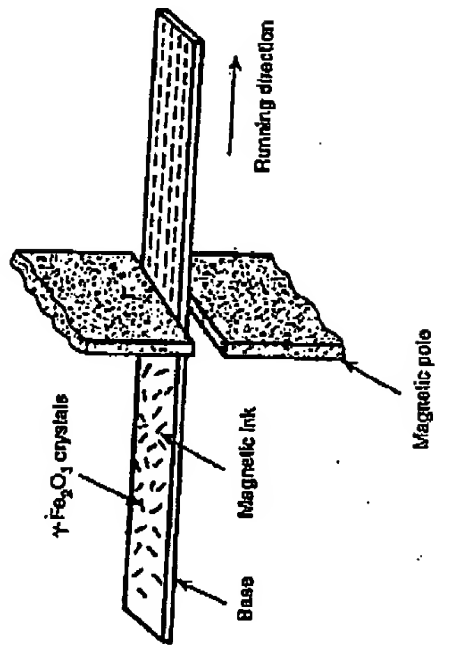
Deposition of solids from the liquid phase 113

through the thermal decomposition and oxidation of needle-like $\alpha\text{-FeOOH}$.

4.3 DEPOSITION OF SOLIDS FROM THE LIQUID PHASE

Most reactions for depositing solid particles from the liquid phase are precipitation reactions of the type $A + B \rightarrow AB$. In this reaction, solid particles of AB are precipitated from the liquid phase (the solution) of two dissolved two components A and B , which are present in the necessary ratio. In order to be able to dissolve ionic compounds with strong interatomic bonding, it is necessary to have solvent molecules that can stabilize dispersed ions by surrounding them with a solvation shell. Solvent molecules with a high permittivity and a strong polarity may be suitable to achieve this stabilization. Molecules such as H_2O and alcohol are good solvents having the necessary properties and are widely used in liquid-phase reactions. Compared with vapour-phase and solid-phase reactions, liquid-phase reactions that precipitate particles by the mixing of two different solutions have the following characteristics:

1. When particles are prepared by precipitation from a multicomponent system, the homogeneity of the components in the solution phase can



of magnetic memory materials. Ferrite, an imperfect spinel form of $\gamma\text{-Fe}_2\text{O}_3$, is used as the magnetic layer on magnetic tape. The ferrite is required as single-domain, needle-like crystals because the coercivity H_c depends exclusively on the anisotropy of crystal shape. One side of a polyester film is coated with a liquid coating containing 0.5 μm long, needle-like crystals of $\gamma\text{-Fe}_2\text{O}_3$. For use in magnetic recording it is necessary that the crystals on the tape are aligned in a specific direction, and this is done by passing the tape through a magnetic field, as shown in Fig. 4.19. The ability to orient the $\gamma\text{-Fe}_2\text{O}_3$ crystals as above is very dependent on being able to increase their magnetic properties. It is necessary first to prepare needle-like $\alpha\text{-FeOOH}$ (orthorhombic) crystals as the starting material for needle-like crystals of $\gamma\text{-Fe}_2\text{O}_3$ (cubic). Single-domain $\gamma\text{-Fe}_2\text{O}_3$ particles with their (110) planes oriented in a specific direction can be prepared by retaining the skeletonized structure (see section 2).